Physical Medicine and Rehabilitation – International

Open Access

Austin Publishing Group

Research Article

Alterations in Satellite Cell Differentiation from Young Patients with Cerebral Palsy

Marlies Corvelyn[1]; Domiziana Costamagna[1,2]; Justine Meirlevede[1]; Robin Duelen[1]; Jorieke Deschrevel[3]; Ghislaine Gayan-Ramirez[3]; Hannah De Houwer[4]; Anja Van Campenhout[4,5]; Kaat Desloovere[2]; Maurilio Sampaolesi[1*]

[1]Stem Cell and Developmental Biology, Dept. of Development and Regeneration, KU Leuven, Belgium

[2]Research Group for Neurorehabilitation, Dept. of Rehabilitation Sciences, KU Leuven, Belgium

[3]Laboratory of Respiratory Diseases and Thoracic Surgery, Dept. of Chronic Diseases and Metabolism, KU Leuven, Belgium

[4]Department of Orthopaedic Surgery, University Hospitals Leuven, Belgium

[5]Department of Development and Regeneration, KU Leuven, Belgium

***Corresponding author: Maurilio Sampaolesi**

Stem Cell and Developmental Biology, Department of Development and Regeneration, KU Leuven, Belgium.

Tel: +3216373132

Email: maurilio.sampaolesi@kuleuven.be

Received: July 03, 2023

Accepted: July 31, 2023

Published: August 07, 2023

Abstract

Cerebral Palsy (CP) is one of the most common lifelong conditions leading to childhood physical disability, affecting approximately 1.6 in 1000 live births. Literature reported muscle alterations of CP patients in comparison to Typically Developing (TD) children such as fibrotic tissue accumulation and reduced Satellite Cell (SC) numbers with altered fusion capacity. To better understand the observed CP muscle phenotype, we quantified and investigated SC-progenitors of the Medial Gastrocnemius from young patients with CP (n=17, aged 3-9 years, GMFCS levels I-III) and age-matched TD children (n=12). We found an increased myotube diameter and a higher amount of nucleus clusters in CP-derived myotubes compared to TD-derived myotubes. Additionally, these nucleus accumulations were larger and less linear in SCs from children with CP compared to TD. Further, no altered expression levels of multiple genes associated with SC differentiation, fusion and nuclear positioning involved in other muscle disorders have been observed. In conclusion, we unprecedently quantified altered differentiation features of SCs from CP muscles with unaltered gene hallmarks of myopathies. Further research would be needed to elucidate pathophysiological mechanisms related to the altered SC properties observed in CP muscles and its impact on in vivo muscle functioning.

Keywords: Satellite cells; Cerebral palsy; Young patients; Myogenesis; Myotube

Abbreviations: BL: Bilateral; BoNT: Botulinum Neurotoxin A; CP: Cerebral Palsy; DMD: Duchenne Muscular Dystrophy; FACS: Fluorescent Activated Cell Sorting; FI: Fusion Index; F: Female; GMFCS: Gross Motor Function Classification System; IF: Immunofluorescent; IQR: Interquartile Range; M: Male; MG: Medial Gastrocnemius; MyHC: Myosin Heavy Chain; RMSE: Rooth Mean Square Error; SC: Satellite Cell; SD: Standard Deviation; ST: Semitendinosus; TD: Typically Developing; UL: Unilateral

Introduction

Cerebral Palsy (CP) is one of the most common lifelong conditions leading to childhood physical disability, with an incidence of around 1.6 in 1000 live births [1]. CP originates from a neural lesion in the immature brain, leading to progressive musculoskeletal symptoms. Clinically, CP manifests itself on both neural and muscular level (spasticity, muscle weakness and decreased muscular control), resulting in decreased functional ability such as disturbed gait [2-4]. These patients can be classified following the Gross Motor Function Classification System (GMFCS), from levels I to V, based on their functional abilities [5,6]. The lower the level the more functional the child is. Treatment mainly consists of management of the symptoms at the muscle level, including physiotherapy, orthoses, Botulinum Neurotoxin A (BoNT) injections and orthopaedic surgery [4,7].

Previous investigations on CP microscopic muscle properties reported altered muscle composition with i.e. an increased collagen content, accumulation of adipose tissue [8-10] and a significant reduction in the number of Satellite Cells (SCs) in contractured muscles of patients with CP [11-13]. SCs are quiescent adult stem cells located between the sarcolemma and the basal lamina of the muscle and are primarily involved in adult myogenesis [14,15]. Unfortunately, research on the functionality of SCs in CP muscle pathology is scarce [16,17] and requires

Citation: Corvelyn M, Costamagna D, Meirlevede J, Duelen R, Deschrevel J, et al. Alterations in Satellite Cell Differentiation from Young Patients with Cerebral Palsy. Phys Med Rehabil Int. 2023; 10(2): 1217.

further examinations. Domenighetti et al. described lower Fusion Index (FI) values in myotubes from CP-derived SCs (patients aged 3-18 years) compared to TD adolescent cells (aged 14-18 years), based on hamstring biopsies [16,18]. Furthermore, they described these myotubes as thinner and more spindle-shaped compared to those of TD adolescents. Our group previously reported higher FI values based on Myosin Heavy Chain (MyHC) expression of SCs from younger patients with CP (aged 3-9 years) derived from microbiopsies of the *Medial Gastrocnemius* (MG) compared to aged-matched TD children [17]. These SC-derived myotubes from children with CP seemed to be larger and contained more accumulations of myonuclei within the myotubes compared to those of TD children. Interestingly, studies regarding other myopathologies, such as facioscapulohumeral and Duchenne Muscular Dystrophies (DMD), have described similar *in vitro* SC alterations in myotube morphology, diameter and/or branching [19-22]. Moreover, also nuclear positioning within the myotube seemed to be pivotal, as impairments in these processes were associated with centronuclear myopathies or Emery-Dreifuss muscular dystrophy [23,24]. These studies while linking *in vitro* SC features to muscle weakness emphasize the relevance of the SC alterations in myotube morphology. Whether the *in vitro* SC-derived myotube alterations can be linked to muscle alterations in CP children is not yet known. This is for a part due to the fact that the measurements up to now were purely descriptive. We, however, believe that the quantification of the myotubes and myonucleus features *in vitro* would help providing a more complete picture of the SC behaviour alterations, ultimately leading to better understanding of the observed muscle alterations. In this regard, Kahn and colleagues also hypothesised altered SC behaviour based on *ex vivo* muscle sections via differences in myonuclear domain in contractured muscles from patients with CP [25].

The current study aimed to employ a software tool developed in our laboratory [26] to quantify the SC-derived myotube phenotype from two different muscles in young patients with CP in comparison to age-matched TD children. We also examined potential associations with clinical parameters and performed explorative assessments of gene expression to determine potentially involved actors in altered SC functioning.

Materials and Methods

Muscle Microbiopsy Collection

This study protocol was approved by the Ethical Committee of the University Hospitals of Leuven, Belgium (S61110 and S62645). Written informed consent was provided by the parents or next of kin. Children with CP were recruited from the CP Reference Centre, whereas TD children were recruited from the Traumatology Unit for upper limb surgeries, or from the Ear, Nose and Throat Unit for other procedures at the University Hospitals Leuven (Belgium). A group of patients with CP (n=17, age 3-9 years; GMFCS I-III) and age-matched TD children (n=12) were included in this study (Table 1). In- and exclusion criteria for both the CP and the TD groups were as described before [17]. All biopsies were collected during interventions requiring general anaesthesia related to orthopaedic interventions (including BoNT-injections). Microbiopsies from the muscle midbelly of the MG were obtained from all enrolled children, while for a subgroup of subjects (CP: n=6, TD: n=3) also a second biopsy of the *Semitendinosus* (ST) was collected. The biopsy collections were performed percutaneously under ultrasound guidance, with a microbiopsy needle (16-gauge, Bard) as described previously [17].

Clinical Outcome Parameters Regarding Muscle Spasticity and Strength in CP Children

The clinical symptoms of the plantar flexors were defined through manual assessments, using the Modified Ashworth Scale to classify spasticity [27] and the Medical Research Council grade scale to classify strength [28]. These clinical assessments were performed by experienced clinicians usually up to 3 months prior to the biopsy collection. To allow simple linear regression analysis, these clinical scores were converted to numerical values: the Modified Ashworth scores 0, 1, 1+, 2, 3 and 4 were transformed towards 0, 1, 2, 3, 4, 5, respectively (whereby 0 = no spasticity); the optional strength scores with a '+' or '-' sign were transformed towards the decimal .5 (for example 2+ and 3- became 2.5) (whereby 5 = no strength impairment).

Cell Culture and Stem Cell Isolation via FACS

For each muscle biopsy, cells were amplified and isolated according to a previous published protocol [17]. In short, cells were amplified till isolation by Fluorescent Activated Cell Sorting (FACS) using a BD FACSAria II (BD biosciences) or Sony MA9000 (Sony) device. Calcein violet (10µM/1x10^6 cells, eBioscience) was used as additional viability control. SC-like progenitors were sorted based on CD56 marker (APC, 0.1µL/1.10^6 cells, Biolegend) as previously described [17,29].

Stem Cell Characterization by Flow Cytometry Analysis

Antibody titrations for FACS optimization and further flow cytometry analyses were performed with a FACSCanto II HTS (BD biosciences). FACS single cell gating was performed through forward and side scatter plots, excluding non-viable cells based on dimension and granularity. Finally, to assess correct gating, bare cells and fluorescent minus one-samples were used. Markers CD56 and CD82 (PE, 0.1µL/1.10^6 cells, Biolegend) were included. Data were analysed with FlowJo v10.6.1 software.

In vitro Differentiation Assays

Myogenic differentiation assays were performed as previously reported [17]. Cells were fixed with 4% paraformaldehyde after 3 days of myogenic differentiation for optimal visualization of the myotubes. SCs for RT-qPCR analyses were cultured in 6-well dishes and differentiated for 6 days to reach maximal maturity.

In vitro Proliferation Assays

Unsorted cells were seeded in duplicate at a density of 13 000/cm^2 in multi-well plates. Cells were grown as described before [17]. Cells were detached using TrypLE™ Express (Thermo Fisher Scientific) at 24, 48 and 72h after seeding and counted using a Countess II (Thermo Fisher Scientific) device. For practical reasons, these experiments were performed on a smaller subgroup of patients with CP and age-matched TD children for the MG (n=6).

Immunofluorescent Staining and Imaging of Differentiated Cells

Immunofluorescent (IF) staining was performed according to our previously published protocol [17]. SCs were stained for MyHC (MF20 (mouse) monoclonal antibody, 1:20, Hybridoma Bank), followed by the appropriate secondary antibody (1:500, Alexa Fluor® donkey 594, Thermo Fisher Scientific). Hoechst (1:3000 in PBS, Thermo Fisher Scientific) was used for indicating nuclei. Visualization occurred with an Eclipse Ti Microscope (Nikon) and NIS-Elements AR 4.11 software.

Table 1: Demographic and anthropometric data for recruited subjects.

MG		TD (N=12)	CP (N=17)			
			Total (N=17)	GMFCS I (N=5)	GMFCS II (N=7)	GMFCS III (N=5)
Age (year)	Mean (SD) Range	5.8 (1.5) 3.4 – 8.6	6.6 (1.8) 3.1 – 8.9	5.9 (1.9) 3.1 – 7.5	6.7 (1.7) 3.7 – 8.9	6.5 (1.8) 6.3 – 8.9
Sex (M – F)	N	8 – 4	11 – 6	3 – 2	6 – 1	2 – 3
Body mass (KG)	Mean (SD)	19.6 (2.6)	21.7 (5.9)	18.9 (3.7)	21.6 (5.3)	21.6 (6.2)
Height (CM)	Mean (SD)	115.1 (8.5)	115.0 (15.6)	108.9 (12.5)	117.6 (15.8)	113.2 (15.3)
Topographic class (UL - BL)	N	-	4 – 13	3 – 2	1 – 6	0 – 7
Number previous BoNT injections MG (N)	Mean (SD) Range	- - -	1.8 (2) 0 – 7	1.7 (1.9) 0 – 3	2.7 (2.6) 0 – 7	1.4 (1.6) 0 – 2
Modified Ashworth plantar flexors	Median Range	- -	2 1 - 3	2 2 - 3	2 1 - 2	3 1.5 - 3
Strength plantar flexors °	Median Range	- -	3.5 1 - 5	3.5 2.5 - 5	3.5 ° 2.5 – 3.5	2.5 ° 1 – 3.5
ST		**TD (N=3)**	**CP (N=6)**			
			Total (N=6)	**GMFCS I (N=0)**	**GMFCS II (N=5)**	**GMFCS III (N=1)**
Age (year)	Mean (SD) Range	6.4 (1.2) 5.6 – 7.8	7.0 (1.3) 5.3 – 8.9	- - -	7.3 (1.3) 5.3 – 8.9	6.9 (-) -
Sex (M – F)	N	2 – 1	4 - 2	-	4 - 1	0 - 1
Body mass (KG)	Mean (SD)	18.0 (3)	23.0 (3.3)	-	23.3 (3.6)	21.5 (-)
Height (CM)	Mean (SD)	119.7 (3.2)	123.4 (10.9)	-	124.3 (11.9)	119.0 (-)
Topographic class (UL - BL)	N	-	0 - 6	-	0 - 5	0 - 1
Number previous BoNT injections ST (N)	Mean (SD) Range	- - -	2.7 (2.4) 1 – 7	- - -	2.8 (2.7) 1 – 7	2 - -

CP: cerebral palsy, TD: typically developing, N: number, GMFCS: Gross motor function classification scale, M: male, F: female, KG: kilogram, CM: centimeter, UL: unilateral, BL: bilateral, BoNT: Botulinum Neurotoxin A, MG: Medial Gastrocnemius, ST: Semitendinosus, SD: standard deviation
No clinical output parameters for the ST are listed, as this dataset was included for explorative purposes
° Strength scores of plantar flexors: 2 datapoints are missing for CP patients with GMFCS II, 1 data point is missing CP patient GMFCS II

Quantitative Satellite Cell Differentiation Outcome Parameters on Myotube Morphology and Nuclear Positioning

Three randomized IF images per well were analysed per assessment. Fusion Index (FI) was calculated as ratio between at least 2 myonuclei per MyHC positive area and the total number of nuclei in a field of view, using ImageJ software. Other parameters assessing myotube morphology and nuclear positioning were obtained via custom-made semi-automatic available software as published by Noë et al. [26]. Three parameters for myotube morphology and three parameters regarding nuclear positioning were defined based on output images as illustrated in Figure 1. First, regarding myotube morphology, the myotube coverage describes the magnitude of all myotubes and is expressed as a percentage of the total field of view. Secondly, myotube diameter was defined as the average based on 5 representative diameters of the 5 largest myotubes per IF image. Thirdly, branching points were defined based on the myotube skeleton and were included if the branch contained at least one nucleus. In regard to nucleus positioning, firstly, the amount of nucleus clusters per field of view was quantified. Nucleus clusters were defined as a group of at least 4 nuclei within a MyHC positive area, with a maximum distance of 4µm, based on an average nucleus diameter of 13µm. Secondly, the Root Mean Square Error (RMSE) values indicate the linearity of nucleus clusters, whereby a higher the value, expressed in µm, points towards a lower linearity. Thirdly, the size of nucleus clusters was subcategorised based on the number of nuclei per cluster (small: 4-9 nuclei, middle: 10-14 nuclei and large: >14 nuclei).

Quantitative RT-qPCR Outcomes Pursuing Myogenic Differentiation, Fusion and Nuclear Positioning

RNA isolation of MG-derived SCs was carried out using the PureLink® RNA Mini Kit (Thermo Fisher Scientific) according to the provided protocol. Genomic DNA traces were removed using Turbo DNase (Thermo Fisher Scientific), following the manufacturer's instructions. RNA concentration was quantified by Spectrophotometer ND-1000 (Nanodrop). First strand cDNA synthesis was carried out based on 200ng of total RNA following the protocol provided by the Superscript III First-Strand Synthesis SuperMix for RT-qPCR kit (Thermo Fisher Scientific). RT-qPCR was performed as described previously [17] using the primers listed in Supplementary table 1. Gene expression levels were normalised to Housekeeping Gene (HKG) β-ACTIN and GAPDH. Delta CT was obtained by subtracting the CT value of the gene of interest from the CT value of the HKGs.

Data Analyses

Data in this study are represented using means ± Standard Deviation (SD) as most parameters are normally distributed, unless stated otherwise. The individual values were indicated in graphs and bars represent the mean. Initially, unpaired T-tests were performed for comparison between the CP and TD groups (two-tailed, $p<0.05$) for both SC differentiation outcomes as well as for the RT-qPCR data. Secondly, one-way ANOVA with Tukey's correction for multiple testing was applied to compare the quantitative SC differentiation outcome parameters from patients with CP, subdivided per GMFCS level and data from TD children. Comparison of RMSE values of all nucleus clusters between CP and TD was performed using a Mann-Whitney test, as these data were not normally distributed. The median and Interquartile Range (IQR) is indicated. Accordingly, a Kruskal-Wallis test was performed to compare CP patients with different GMFCS levels and TD for this RMSE parameter. A chi-squared test was applied for assessing differences on the size of the nucleus clusters between TD and CP. Sample sizes of the analysed data are always indicated in the results section, as well as in the figure legends. Statistical analysis was performed using GraphPad Prism 8 software (version 8.4.3). Significance levels of $p=0.05$ were indicated by '*'.

Results

Muscle Cell Proliferation and Characterization

Proliferation rates from all MG-derived muscle cells of patients with CP, GMFCS levels II-III, were determined via doubling time assessments (Figure 2A). Slightly lower doubling times over a time course of 48h were observed for CP (27.19±4.25h, n=5) compared to TD (30.77±5.13h, n=6) muscle cells, although not significant. No significant differences were found after the first 24h (24-48h), while in the second 24h (48h-72h) the doubling time of the cells derived from CP children was significantly shorter compared to those of TD children (data not shown).

Flow cytometry analysis showed no differences in CD82 protein levels, a regulator of SC proliferation-differentiation [30], between cells derived from CP MG muscle compared to the ones from TD (Figure 2B, C). Additionally, the purity of SCs based on a co-localization of CD56 and CD82 was of 87.24±11.18% (TD: n=6, CP: n=6).

Phenotype of Differentiated Satellite Cells from MG of Patients with CP

MG-derived SCs from patients with CP (n=17) and TD children (n=12) were differentiated for 3 days and analysed based on MyHC localization. IF images (Figure 3A) revealed a tendency of an increased FI in CP SCs (41.10±12.80%) compared to TD SCs, although not significant (33.16±8.83%, p=0.075) (Figure 3B).

Moreover, using the custom-made semi-automatic Myotube Analyzer tool [26], myotube morphology features were quantified (Figure 3B-E). Myotube coverage in SCs from patients with CP (34.05±10.99%) showed a trend towards an increasement compared to those from TD children (27.25±8.10%, p=0.080). The myotube diameter of the largest myotubes significantly increased in CP compared to TD cells (41.80±11.92µm vs 32.40±6.03µm, respectively; *p<0.05). No differences in the number of branching points of myotubes from CP and TD samples were observed and there were no significant associations between these parameters and the GMFCS levels or BoNT treatment history.

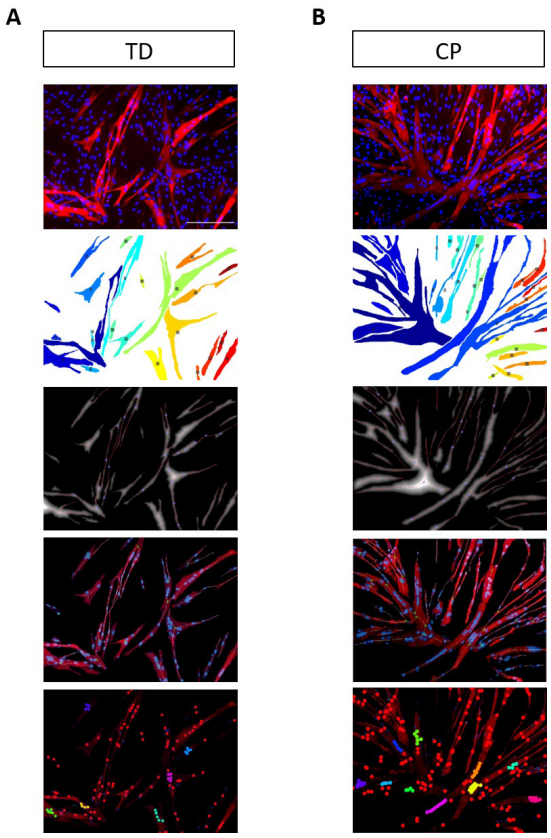

Figure 1: Output images from Myotube Analyzer tool. Example of image analyses for SC differentiation from a Typically Developing (TD) child (A) and child with Cerebral Palsy (CP) (B). From top to bottom: The first images represent the IF input images. MyHC localization is shown in red, nuclei are counterstained in blue using Hoechst. Scale bar is 200µm. Second images are the identification of the different myotubes, used to determine the myotube coverage. Third images are the skeleton image used for diameter assessments (5 representative dots for the 5 largest myotubes are indicated). The grey scale indicates the distance towards the myotube borders, indicating the centre of the myotube in white. The fourth images show the skeleton (white dotted line) on the MyHC expression to aid the user in indicating the myotube branching points (green circles) as previously defined. The fifth images show all the nuclei within the MyHC area (in red). All nuclei that are identified as nucleus clusters are indicated in different colours for visual identification of the different clusters with its features based on RMSE values and magnitude of the nucleus cluster.

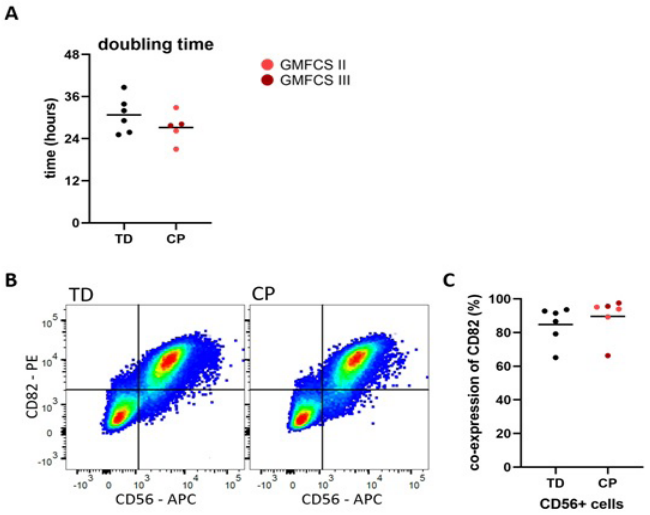

Figure 2: Proliferative capacities of MG-derived cells from CP compared to TD. (A) Doubling time, expressed in hours, is shown for muscle cells from TD children and patients with CP. Every dot represents an individual included subject (TD: n=6, CP: n=5). The horizontal bar indicates the mean. Patients with CP, subcategorized in different GMFCS levels, are represented in different colours, as indicated by the legend. (B) Representative flow cytometry analysis for SC-markers CD82 and CD56 on muscle cells from TD children and patients with CP. (C) Percentages of flow cytometry analysis for co-expression with CD82 as a purity measure for CD56+ cells for TD and CP. Every dot represents an individual subject (TD: n=6, CP: n=6). The horizontal bar indicates the mean. p>0.05.

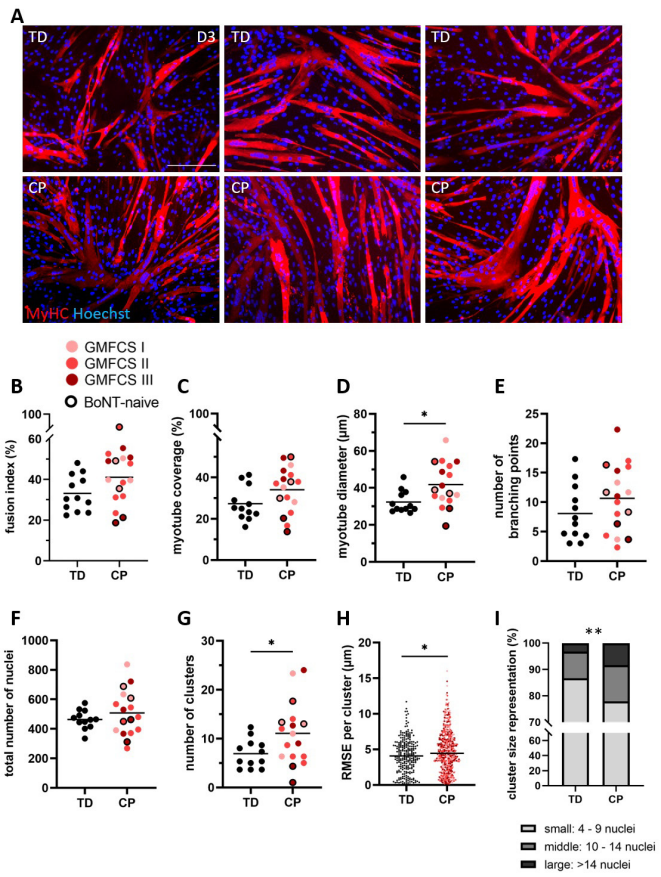

Figure 3: Myotube morphology and nuclear positioning from *Medial Gastrocnemius*-derived satellite cells in CP compared to TD. (A) Representative IF images for SCs after 3 days of myogenic differentiation. SCs from TD children and patients with CP (GMFCS level I, II and III) are shown. MyHC is indicated in red, nuclei are counterstained in blue using Hoechst. Scale bar is 200µm. (B-G) Different parameters assessed based on IF images of these SCs from TD (n=12) and CP (n=17). Every dot represents an individual subject. The horizontal bar indicates the mean. Patients with CP, subcategorized in different GMFCS levels, are represented in different colours. Patients with CP with no treatment history of BoNT are indicated with coloured dots with black outlines. (H) Root mean square error (RMSE) values for all nucleus clusters observed in TD (n=249) and CP (n=564). The bar indicates the median. (I) Bar chart showing the nucleus cluster representation based on the cluster size for TD and CP. *p<0.05, **p<0.01.

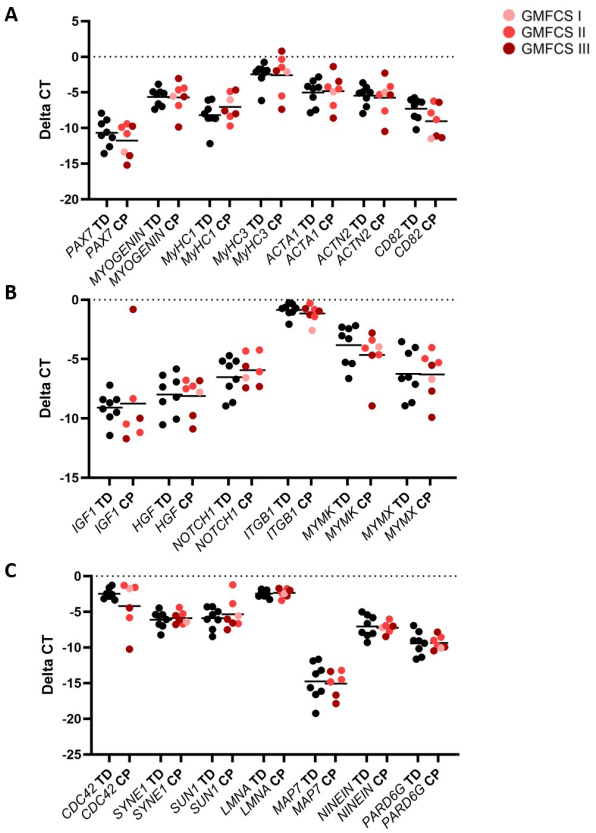

Figure 4: Gene analyses for MG-derived satellite cells from TD and CP after differentiation. RT-qPCR of SCs after 6 days of differentiation for genes involved in (A) differentiation, (B) fusion and (C) nuclear positioning. Expression levels are indicated through delta CT values, normalised against housekeeping genes *b-ACTIN* and *GAPDH*. Every dot represents an individual subject (TD: n=8, CP: n=7). The horizontal bar indicates the mean. Patients with CP, subcategorized in different GMFCS levels, are represented in different colours, as indicated by the legend. p>0.05.

The analysis of the amount of SC nuclei and their positioning within the myotube (Figure 3F-I) revealed that the total number of nuclei per field of view did not differ between CP and TD children (Figure 3F). The average number of nucleus clusters significantly increased in CP (11.06±6.34) compared to TD (6.92±2.94, p<0.05) children (Figure 3G). The RSME value for all nucleus clusters (n=564) from CP SCs had a median value of 4.449µm (IQR: 2.637-6.511), which was significantly higher compared to data of TD SCs (median value of 4.079µm, IQR: 2.392–5.764, n=249, *p<0.05). When subcategorizing the patients with CP per GMFCS level, the median RMSE from patients with GMFCS level I was significantly higher compared to the data of the TD group (p<0.05, data not shown). Further distribution based on the size of the nucleus clusters, showed significantly higher middle (10-14 nuclei) and large (>14 nuclei) sized clusters in CP (13.65% and 8.33%, respectively) compared to TD (10.04% and 3.21%, respectively, **p<0.01) muscles (Figure 3I). No associations between these parameters describing nucleus positioning and GMFCS levels or BoNT treatment history of the patients were found.

Associations between SC Derived from MG with Clinical Outcome Parameters

Significant alterations in SCs from CP compared to TD have been visualised with clinical parameters for spasticity (based on the Modified Ashworth Scale) and strength (Supplementary figure 1). No associations between spasticity or strength and FI values, myotube diameter or number of clusters could be found.

Phenotype of Differentiated Satellite Cells from ST for a Subgroup of Patients with CP

The same parameters as in Figure 3 were also included for SCs derived from the ST muscle from patients with CP (n=6) and TD children (n=3) to preliminary assess muscle-specificity of the observed phenotype (Supplementary figure 2). A similar trend in increased cluster magnitude between CP (11.63% middle-sized clusters, n=86) and TD (8.33% middle-sized clusters, n=36) was observed, although partially hampered due to lower FI values in ST-derived SCs.

Satellite Cell Gene Expression Levels During Differentiation

Gene analysis regarding SC differentiation was performed (Figure 4A). After 6 days of myogenic differentiation, low levels of quiescence marker *PAX7* were reported for both SCs from patients with CP (n=7) and TD children (n=8). *MYOGENIN*, a late-stage transcriptional activator for myogenesis, was similarly expressed between CP and TD. Furthermore, no alterations between CP and TD were found in *MyHC* and *ACTIN* levels, involved genes for contractile protein production. Lastly, *CD82* seemed slightly decreased in CP compared to TD, but failed to reach significance.

Furthermore, different gene targets involved in SC fusion were assessed (Figure 4B). Transcript levels for multiple growth factors, such as *IGF1* and *HGF* were not altered in SCs from CP

compared to TD. Additionally, two key-players in signaling pathways regulating SC self-renewal and differentiation, *NOTCH1* and *ITGB1* also did not show altered levels between CP and TD. *MYMK* and *MYMX*, two crucial genes for myoblast fusion, did not differ between CP and TD. Interestingly, SCs from one specific patient with CP (GMFCS level III) showed particularly high expression of *IGF1*, while the expression of *MYMK* and *MYMX* was strikingly lower compared to the other samples (Supplementary figure 3).

Lastly, multiple genes involved in nuclear positioning within the myotube, better studied in Drosophila, but also often associated with human myopathies, have been assessed (Figure 4C). The expression of *CDC42*, a regulator of actin polymerization aiding intracellular movement, was not altered in SCs from CP compared to TD as were the expressions of *SYNE1* and *SUN1*, two genes associated with the cytoskeleton. *LMNA* gene expression, which is altered in congenital muscular dystrophy and usually associated with muscle weakness, did not differ in SCs from TD or patients with CP. Finally, *MAP7* and *NINEIN*, two genes linked to microtubule polymerization, and *PARD6G*, a gene involved in asymmetrical division and nuclear cluster formation in Drosophila, showed no altered expression levels in SCs from children with CP compared to TD.

Discussion

This study quantitatively described altered differentiation features from MG-derived SCs of children with CP compared to those of TD children. No alterations in CD82 availability were reported, yet these flow cytometry analyses confirmed the purity of the CD56-isolated SCs. After SC differentiation, with respect to myotube morphology, we showed increased myotube diameter in CP myotubes compared to controls. Furthermore, in regard to nuclear positioning, more nucleus clusters with larger and less linear nucleus accumulations in CP-derived myotubes compared to TD-derived myotubes were found. However, none of these differentiation outcome parameters could be associated with clinical measures of muscle spasticity or strength. Gene expression of multiple genes associated with the alterations of SC differentiation, fusion and nuclear positioning in other myopathies were found unaffected in the current CP data.

The tendency of reduced doubling time in SC from patient with CP compared to TD is in line with previous findings of Sibley et al reporting a doubling time around 24h for CP-derived myoblasts and 34h for those from TD from the hamstring muscles [18]. However, this hyperproliferative hallmark has not yet been further investigated to understand its implications on *in vivo* functioning.

Quantitative measurements of SC differentiation features are often lacking, due to insufficiently standardized analysis methods and parameters. However, larger myotubes and altered morphology based on for example branching, have been previously described in other pathologies that are characterized by muscle weakness [19-22]. To date, CP muscle myopathy has been mainly associated with sarcopenia because of the reported muscle wasting and altered extra-cellular matrix deposition [31,32]. Furthermore, based on gene ontology and pathway analyses of publicly available microarray datasets, Von Walden and colleagues showed larger similarities with CP and aged muscles, and thereby sarcopenia, rather than disused muscles [33]. Further validation of the observed *in vitro* CP-phenotype based on *ex vivo* muscle sections, i.e. assessing the myonuclear domain, would better indicate the implications of these findings on the muscles of these patients.

This study further suggests muscle-specificity of the CP pathology for the MG muscle, as the observed phenotype was not confirmed in SCs derived from the ST. Previous published data on CP muscle symptoms and macro- and microscopic features showed to be highly heterogenous depending on the assessed muscle [4]. For example, a broad range of muscle deficits based on muscle volume assessments was shown in the different lower limb muscles of patients with CP [34]. Additionally, in the light of SC muscle functioning, previous reported alterations in fusion capacity have also shown contrasting results, partly due to different assessed muscles [16,17]. Hence caution towards generalized treatment is warranted.

SC functioning and their involvement relies on multiple steps, such as cell activation, proliferation and differentiation [35]. CD82 [30] and NOTCH [36] have been described to be involved in maintaining a proper balance between proliferation and differentiation and the upregulation of NOTCH correlated with muscle fibrosis and the rapid depletion of SCs in a DMD mouse model [37]. Interestingly, these latter events have been reported similarly for patients with CP [11-13]. Next, during regeneration, the process of fusion counts multiple steps such as cell adhesion and pore formation, for which the expression of MYMK and MYMX showed to be crucial [38,39]. Lastly, mainly based on research in Drosophila, the processes of nuclear positioning within the myotube and myofibre were considered crucial in efficient muscle usage [23,40]. In this context, SC dysfunction was found to be associated with multiple (neuro)muscular disorders, the so-called satellite cell-opathies [41]. Therefore, the current study has assessed the gene expression levels of some of the actors involved in these processes with known associations to muscle weakness. For example, mutations in SYNE1 have been linked to a spectrum of neuromuscular diseases, resulting in increased muscle tension and hyperreflexia [42,43]. This latter symptom is often confused with spasticity, which is also one of the main clinical representations in the CP patient population [44]. Additionally, mutations in *LMNA* have been collected under the term of laminopathies and have shown to result in abnormal myotube formation and nuclear behaviour [45]. Unfortunately, the expression of genes analysed in this study did not show any statistical differences between CP and TD. However, as the aetiology and the clinical representation of CP is highly heterogeneous, it is very likely that not just one mechanism is involved in CP muscle pathology. Hence, we have currently only focussed on the involvement of SC-derived myoblasts and not on multiple mediators i.e. via cell signalling or cell-cell interactions. Other studies reported high levels of heterogeneity based on gene expression levels, via micro-arrays or RNA sequencing analysis, showing upregulated pathways of inflammation or ECM production in CP [13,46-49]. Nevertheless, even though the gene targets were carefully selected in this study, high-throughput methods, such as RNA sequencing, would be useful to further investigate the observed phenotype and identify potentially altered pathways.

In conclusion, the current study provided a comprehensive and quantified analysis of SC differentiation features. Specifically, in the context of SCs derived from the MG muscle of young patients with CP, we showed alterations in myotube morphology and nuclear positioning compared to differentiated SCs from age-matched TD children. Furthermore, preliminary assessments of gene expression levels involved in the described SC phenotype have been performed, highlighting the need for

more high-throughput methods and a better patient classification. Further research would be necessary to clarify pathophysiological mechanisms related to the altered SC properties observed in CP muscles.

Author Statements

Supplementary Materials

Table S1: Primer list for RT-qPCR, Figure S1: Satellite cell differentiation features from the MG associated with muscle spasticity and strength, Figure S2: Myotube morphology and nuclear positioning from *Semitendinosus*-derived satellite cells in CP compared to TD, Figure S3: Heatmap representation of RT-qPCR data.

Author Contributions

Conceptualization: all authors; methodology: MC, DC and RD; software: MC, DC and JM.; validation: MC.; formal analysis: MC and JM.; investigation: MC; resources: MC, DC, HDH, AVC, KD and MS; data curation: MC; writing—original draft preparation: MC; writing—review and editing: all authors.; visualization: MC.; supervision: DC, KD and MS; project administration: KD.; funding acquisition: KD. All authors have read and agreed to the published version of the manuscript.

Funding

MS is supported by The Research Foundation Flanders (FWO) (#G066821N), INTERREG – Euregio Meuse-Rhine (GYM, Generate your muscle 2020-EMR116), and the Italian Ministry of Health, Ricerca Finalizzata (RF-2019-12369703).

Institutional Review Board Statement

The study was conducted in accordance with the Declaration of Helsinki, and approved by the Ethical Committee of the University Hospitals of Leuven, Belgium (S61110 and S62645).

Informed Consent Statement

Written informed consent to participate in this study was provided by the participants' legal guardian/next of kin.

Acknowledgments

We warmly thank all children and their families for participating in this study. We are grateful for the contribution of Prof. MD S. Nijs and E. Nijs from the Traumatology Department and Prof. MD G. Hens from the Ear, Nose Throat department for the contribution to the recruitment of TD children, associated to the University Hospital of Leuven, Belgium, as well as all staff involved. Special thanks to J. Uytterhoeven and L. Staut, who supported the recruitment procedure.

Conflicts of Interest

The authors declare that the research was conducted in the absence of any commercial or financial relationships that could be construed as a potential conflict of interest.

References

1. McIntyre S, Goldsmith S, Webb A, Ehlinger V, Hollung SJ, McConnell K, et al. Global prevalence of cerebral palsy: A systematic analysis. Dev Med Child Neurol. 2022; 64: 1494-506.
2. Mathewson MA, Lieber RL. Pathophysiology of muscle contractures in cerebral palsy. Phys Med Rehabil Clin N Am. 2015; 26: 57-67.
3. Romero B, Robinson KG, Batish M, Akins RE. An emerging role for epigenetics in cerebral palsy. J Pers Med. 2021; 11.
4. Howard JJ, Graham K, Shortland AP. Understanding skeletal muscle in cerebral palsy: a path to personalized medicine? Dev Med Child Neurol. 2022; 64: 289-95.
5. Palisano R, Rosenbaum P, Walter S, Russell D, Wood E, Galuppi B. Development and reliability of a system to classify gross motor function in children with cerebral palsy. Dev Med Child Neurol. 1997; 39: 214-23.
6. Palisano RJ, Rosenbaum P, Bartlett D, Livingston MH. Content validity of the expanded and revised Gross Motor Function Classification System. Dev Med Child Neurol. 2008; 50: 744-50.
7. Novak I. Evidence-based diagnosis, health care, and rehabilitation for children with cerebral palsy. J Child Neurol. 2014; 29: 1141-56.
8. Johnson DL, Miller F, Subramanian P, Modlesky CM. Adipose tissue infiltration of skeletal muscle in children with cerebral palsy. J Pediatr. 2009; 154: 715-20.
9. Smith LR, Lee KS, Ward SR, Chambers HG, Lieber RL. Hamstring contractures in children with spastic cerebral palsy result from a stiffer extracellular matrix and increased in vivo sarcomere length. J Physiol. 2011; 589: 2625-39.
10. Howard JJ, Herzog W. Skeletal muscle in cerebral palsy: from belly to myofibril. Front Neurol. 2021; 12: 620852.
11. Smith LR, Chambers HG, Lieber RL. Reduced satellite cell population may lead to contractures in children with cerebral palsy. Dev Med Child Neurol. 2013; 55: 264-70.
12. Dayanidhi S, Dykstra PB, Lyubasyuk V, McKay BR, Chambers HG, Lieber RL. Reduced satellite cell number in situ in muscular contractures from children with cerebral palsy. J Orthop Res. 2015; 33: 1039-45.
13. Von Walden F, Gantelius S, Liu C, Borgström H, Björk L, Gremark O, et al. Muscle contractures in patients with cerebral palsy and acquired brain injury are associated with extracellular matrix expansion, pro-inflammatory gene expression, and reduced rRNA synthesis. Muscle Nerve. 2018; 58: 277-85.
14. Fu X, Wang H, Hu P. Stem cell activation in skeletal muscle regeneration. Cell Mol Life Sci. 2015; 72: 1663-77.
15. Bachman JF, Chakkalakal JV. Insights into muscle stem cell dynamics during postnatal development. FEBS Journal. 2021:1-13.
16. Domenighetti AA, Mathewson MA, Pichika R, Sibley LA, Zhao L, Chambers HG, et al. Loss of myogenic potential and fusion capacity of muscle stem cells isolated from contractured muscle in children with cerebral palsy. Am J Physiol Cell Physiol. 2018; 315: C247-57.
17. Corvelyn M, De Beukelaer N, Duelen R, Deschrevel J, Van Campenhout A, Prinsen S, et al. Muscle microbiopsy to delineate stem cell involvement in young patients: A novel approach for children with cerebral palsy. Front Physiol. 2020; 11: 945.
18. Sibley LA, Broda N, Gross WR, Menezes AF, Embry RB, Swaroop VT, et al. Differential DNA methylation and transcriptional signatures characterize impairment of muscle stem cells in pediatric human muscle contractures after brain injury. FASEB J. 2021; 35: e21928.
19. Barro M, Carnac G, Flavier S, Mercier J, Vassetzky Y, Laoudj-Chenivesse D. Myoblasts from affected and non-affected FSHD muscles exhibit morphological differentiation defects. J Cell Mol Med. 2010; 14: 275-89.
20. Pomiès P, Rodriguez J, Blaquière M, Sedraoui S, Gouzi F, Carnac

G, et al. Reduced myotube diameter, atrophic signalling and elevated oxidative stress in cultured satellite cells from COPD patients. J Cell Mol Med. 2015; 19: 175-86.

21. Chal J, Oginuma M, Al Tanoury Z, Gobert B, Sumara O, Hick A, et al. Differentiation of pluripotent stem cells to muscle fiber to model Duchenne muscular dystrophy. Nat Biotechnol. 2015; 33: 962-9.

22. Fernandes SA, Almeida CF, Souza LS, Lazar M, Onofre-Oliveira P, Yamamoto GL, et al. Altered in vitro muscle differentiation in X-linked myopathy with excessive autophagy. Dis Model Mech. 2020; 13.

23. Folker ES, Baylies MK. Nuclear positioning in muscle development and disease. Front Physiol. 2013; 4: 363.

24. Azevedo M, Baylies MK. Getting into position: nuclear movement in muscle cells. Trends Cell Biol. 2020; 30: 303-16.

25. Kahn RE, Krater T, Larson JE, Encarnacion M, Karakostas T, Patel NM, et al. Resident muscle stem cell myogenic characteristics in postnatal muscle growth impairments in children with cerebral palsy. Am J Physiol Cell Physiol. 2023; 324: C614-31.

26. Noë S, Corvelyn M, Willems S, Costamagna D, Aerts JM, Van Campenhout A, et al. The Myotube Analyzer: how to assess myogenic features in muscle stem cells. Skelet Muscle. 2022; 12: 12.

27. Bohannon RW, Smith MB. Interrater reliability of a modified Ashworth scale of muscle spasticity. Phys Ther. 1987; 67: 206-7.

28. Bohannon RW. Considerations and practical options for measuring muscle strength: A narrative review. BioMed Res Int. 2019; 2019: 8194537.

29. Illa I, Leon-Monzon M, Dalakas MC. Regenerating and denervated human muscle fibers and satellite cells express neural cell adhesion molecule recognized by monoclonal antibodies to natural killer cells. Ann Neurol. 1992; 31: 46-52.

30. Hall A, Fontelonga T, Wright A, Bugda Gwilt K, Widrick J, Pasut A, et al. Tetraspanin CD82 is necessary for muscle stem cell activation and supports dystrophic muscle function. Skelet Muscle. 2020; 10: 34.

31. Verschuren O, Smorenburg ARP, Luiking Y, Bell K, Barber L, Peterson MD. Determinants of muscle preservation in individuals with cerebral palsy across the lifespan: a narrative review of the literature. J Cachexia Sarcopenia Muscle. 2018; 9: 453-64.

32. Handsfield GG, Williams S, Khuu S, Lichtwark G, Stott NS. Muscle architecture, growth, and biological Remodelling in cerebral palsy: a narrative review. BMC Musculoskelet Disord. 2022; 23: 233.

33. von Walden F, Vechetti IJ, Englund D, Figueiredo VC, Fernandez-Gonzalo R, Murach K, et al. Reduced mitochondrial DNA and OXPHOS protein content in skeletal muscle of children with cerebral palsy. Dev Med Child Neurol. 2021; 63: 1204-12.

34. Noble JJ, Fry NR, Lewis AP, Keevil SF, Gough M, Shortland AP. Lower limb muscle volumes in bilateral spastic cerebral palsy. Brain Dev. 2014; 36: 294-300.

35. Snijders T, Nederveen JP, McKay BR, Joanisse S, Verdijk LB, van Loon LJC, et al. Satellite cells in human skeletal muscle plasticity. Front Physiol. 2015; 6: 1-21.

36. Luo D, Renault VM, Rando TA. The regulation of Notch signaling in muscle stem cell activation and postnatal myogenesis. Semin Cell Dev Biol. 2005; 16: 612-22.

37. Mu X, Tang Y, Lu A, Takayama K, Usas A, Wang B, et al. The role of Notch signaling in muscle progenitor cell depletion and the rapid onset of histopathology in muscular dystrophy. Hum Mol Genet. 2015; 24: 2923-37.

38. Murach KA, Fry CS, Dupont-Versteegden EE, McCarthy JJ, Peterson CA. Fusion and beyond: satellite cell contributions to loading-induced skeletal muscle adaptation. FASEB J. 2021; 35: e21893.

39. Zhang H, Wen J, Bigot A, Chen J, Shang R, Mouly V, et al. Human myotube formation is determined by MyoD–Myomixer/Myomaker axis. Sci Adv. 2020; 6: 1-14.

40. Roman W, Gomes ER. Nuclear positioning in skeletal muscle. Semin Cell Dev Biol. 2018; 82: 51-6.

41. Ganassi M, Zammit PS. Involvement of muscle satellite cell dysfunction in neuromuscular disorders: expanding the portfolio of satellite cell-opathies. Eur J Transl Myol. 2022; 32.

42. Baumann M, Steichen-Gersdorf E, Krabichler B, Petersen BS, Weber U, Schmidt WM, et al. Homozygous SYNE1 mutation causes congenital onset of muscular weakness with distal arthrogryposis: a genotype–phenotype correlation. Eur J Hum Genet. 2017; 25: 262-6.

43. Wiethoff S, Hersheson J, Bettencourt C, Wood NW, Houlden H. Heterogeneity in clinical features and disease severity in ataxia-associated SYNE1 mutations. J Neurol. 2016; 263: 1503-10.

44. Bar-On L, Molenaers G, Aertbeliën E, Van Campenhout A, Feys H, Nuttin B, et al. Spasticity and its contribution to hypertonia in cerebral palsy. BioMed Res Int. 2015; 2015: 317047.

45. Steele-Stallard HB, Pinton L, Sarcar S, Ozdemir T, Maffioletti SM, Zammit PS, et al. Modeling skeletal muscle laminopathies using human induced pluripotent stem cells carrying pathogenic LMNA mutations. Front Physiol. 2018; 9: 1332.

46. Smith LR, Chambers HG, Subramaniam S, Lieber RL. Transcriptional abnormalities of hamstring muscle contractures inChildren with cerebral palsy. PLOS ONE. 2012; 7: 40686.

47. Smith LR, Pontén E, Hedström Y, Ward SR, Chambers HG, Subramaniam S, et al. Novel transcriptional profile in wrist muscles from cerebral palsy patients. BMC Med Genomics. 2009; 2: 44.

48. Robinson KG, Crowgey EL, Lee SK, Akins RE. Transcriptional analysis of muscle tissue and isolated satellite cells in spastic cerebral palsy. Dev Med Child Neurol. 2021; 63: 1213-20.

49. Pingel J, Kampmann ML, Andersen JD, Wong C, Døssing S, Børsting C, et al. Gene expressions in cerebral palsy subjects reveal structural and functional changes in the gastrocnemius muscle that are closely associated with passive muscle stiffness. Cell Tissue Res. 2021; 384: 513-26.